



UNIVERSITY OF LEEDS

This is a repository copy of *Structural evidence for solvent-stabilisation by aspartic acid as a mechanism for halophilic protein stability in high salt concentrations.*

White Rose Research Online URL for this paper:  
<http://eprints.whiterose.ac.uk/101531/>

Version: Accepted Version

---

**Article:**

Lenton, S, Walsh, DL, Rhys, NH et al. (2 more authors) (2016) Structural evidence for solvent-stabilisation by aspartic acid as a mechanism for halophilic protein stability in high salt concentrations. *Physical Chemistry Chemical Physics*, 18 (27). pp. 18054-18062. ISSN 1463-9076

<https://doi.org/10.1039/c6cp02684b>

---

© the Owner Societies 2016 (Royal Society of Chemistry). This is an author produced version of a paper published in *Physical Chemistry Chemical Physics*. Uploaded in accordance with the publisher's self-archiving policy.

**Reuse**

Unless indicated otherwise, fulltext items are protected by copyright with all rights reserved. The copyright exception in section 29 of the Copyright, Designs and Patents Act 1988 allows the making of a single copy solely for the purpose of non-commercial research or private study within the limits of fair dealing. The publisher or other rights-holder may allow further reproduction and re-use of this version - refer to the White Rose Research Online record for this item. Where records identify the publisher as the copyright holder, users can verify any specific terms of use on the publisher's website.

**Takedown**

If you consider content in White Rose Research Online to be in breach of UK law, please notify us by emailing [eprints@whiterose.ac.uk](mailto:eprints@whiterose.ac.uk) including the URL of the record and the reason for the withdrawal request.



[eprints@whiterose.ac.uk](mailto:eprints@whiterose.ac.uk)  
<https://eprints.whiterose.ac.uk/>

# 1 Structural evidence for solvent-stabilisation by aspartic acid as a 2 mechanism for halophilic protein stability in high salt concentrations

3 Samuel Lenton,<sup>a,b</sup> Danielle L. Walsh,<sup>a,b</sup> Natasha H. Rhys,<sup>a</sup> Alan K. Soper<sup>c</sup> and Lorna Dougan<sup>\*a,b</sup>

4 Halophilic organisms have adapted to survive in high salt environments, where mesophilic organisms would perish. One of the biggest  
5 challenges faced by halophilic proteins is the ability to maintain both structure and function under molar concentrations of salt. A distinct  
6 adaptation of halophilic proteins, compared to mesophilic homologues, is the abundance of aspartic acid on the protein surface.  
7 Mutagenesis and crystallographic studies of halophilic proteins suggest an important role for solvent interactions with the surface aspartic  
8 acid residues. This interaction, between the regions of acidic protein surface and solvent, is thought to maintain a hydration layer around  
9 the protein under molar salt concentrations thereby allowing halophilic proteins to retain their functional state. Here we present neutron  
10 diffraction data of monomeric zwitterionic form of aspartic acid solutions at physiological pH in 0.25 M and 2.5 M concentration of  
11 potassium chloride, to mimic mesophilic and halophilic-like environmental conditions. We have used isotopic substitution in combination  
12 with empirical potential structure refinement to extract atomic-scale information from the data. Our study provides structural insight that  
13 support the hypothesis that carboxyl groups on acidic residues bind water more tightly under high salt conditions, in support of the  
14 residue-ion interaction model of halophilic protein stabilisation. Furthermore our data show that in the presence of high salt the self  
15 association between the zwitterionic form of aspartic acid molecules is reduced, suggesting a possible mechanism through which protein  
16 aggregation is prevented.

## 17 Introduction

18 Extremophilic organisms have adapted to survive extreme environments including extremes of temperature,  
19 pressure and salinity. These remarkable organisms do not merely survive but rather thrive under conditions which  
20 were, until recently, thought of as inimical to life<sup>1-3</sup>. In the case of extreme salinity, halophilic organisms have  
21 adapted to survive and replicate in environments containing molar concentrations of salt<sup>4,5</sup>. Survival in such briny  
22 environments is challenging mainly due to a reduction in the amount of biologically available water. This  
23 availability, in the form of a water solvation layer around proteins, is critical for biological activity, which is in part  
24 why mesophilic proteins are often unstable in high salt conditions<sup>6-9</sup>. Despite this challenge and others associated  
25 with high salt concentrations, all three domains of life have developed evolutionary strategies to survive under  
26 extreme molar salt conditions<sup>5,10</sup>. Halobacteria, such as *Halobacterium Salinarium*, are a distinct evolutionary  
27 branch of the archaea found in water saturated or nearly saturated with salt<sup>11</sup>. Survival of halobacteria under  
28 molar salt conditions is in part facilitated by the presence of bacteriorhodopsin in the cell membrane<sup>12</sup>.  
29 Bacteriorhodopsin regulates the intracellular ion concentration by pumping out sodium across a proton gradient  
30 resulting in high intracellular concentrations of potassium ions<sup>13</sup>. The resulting accumulation of potassium ions in  
31 the cytoplasm requires modifications of intracellular proteins so that they can retain their function<sup>14</sup>. Several  
32 characteristic modifications of proteins from halobacteria have been observed including a reduction of lysine  
33 residues, a relatively low hydrophobic core, an increase in loops and the presence of a large amount of acidic  
34 residues, including glutamic acid and aspartic acid, on the protein surface<sup>15-18</sup>. The first of these two features are  
35 thought to be well understood. In molar salt concentrations of salt proteins will have an increase in hydrophobic  
36 interactions, leading to aggregation resulting from interactions of hydrophobic patches on a protein's surface and  
37 a decrease in the flexibility of the protein core. In order to prevent aggregation, it is important to reduce exposed  
38 hydrophobic surfaces, which is achieved through a reduction in the number of lysine residues. Protein flexibility is  
39 important for activity, and the reduction of large hydrophobic residues may play an important role.

40  
41 The increased number of acidic residues on the surface of halophilic proteins has been interpreted in a number of  
42 different ways and consequently the role of these acidic residues in halophilic protein stability and flexibility is less  
43 clear. Studies have suggested they are important for binding of water molecules, specific binding of ions,  
44 preventing aggregation through repulsive interactions and maintaining flexibility within a protein. Here we  
45 highlight a number of recent studies. Tadeo *et al* showed that obligate halophiles can be created from mesophilic  
46 proteins by mutation of only a few surface residues to aspartic acid<sup>19,20</sup>. This work demonstrated complete  
47 preservation of the three-dimensional structure of the mutated protein and measure increase in thermodynamic  
48 stability achieved for each addition of a surface aspartic acid residue. These studies that the preference for  
49 shorter side-chain residues, such as aspartic acid, on the protein surface results in increased hydrophobic packing  
50 and a decreased surface tension, thereby increasing stability<sup>20</sup>. However, earlier work by Razvi & Scholtz  
51 suggested that the charge, rather than length, of exposed acidic amino acid residues is a greater determiner of  
52 halophilic protein stability<sup>21</sup>. Studies by Zaccai *et al* have shown that halophilic proteins bind significant numbers

of salt molecules, suggesting that the acidic residues are important for binding a large network of hydrated salt ions. This preferential recruitment of salt ions may then be better able to maintain a hydration layer under high salt conditions<sup>19, 22</sup>. However, while the binding of ions to the negatively charged surface has been observed in crystallographic structures of halophilic proteins other studies have failed to show large numbers of ions<sup>23-25</sup>. This discrepancy could be due to the requirement of specific additives in the crystallogenesi process aimed at crystal growth rather than representing *in vivo* conditions. Solvent molecules present on the surface may be an artefact of the crystallisation process; therefore caution has to be taken when making an inference from this type of data<sup>24, 26, 27</sup>. Nevertheless, there is ample evidence for binding of salt ions to some halophilic proteins, indicating that these proteins harness the high ionic strength of their environment rather than being protected from it. While the most prevalent adaptations observed for halophilic proteins is the abundance of acidic residues on the surface of the protein, much interest remains in determining the functions of these acidic residues, including binding of essential water molecules, specific binding of salt and prevention of aggregation.

To further determine the specific function of aspartic acid on the surface of halophilic proteins we have used total neutron diffraction in combination with empirical potential structure refinement (EPSR). This technique provides atomic-scale insight into the structure and interactions of amorphous solutions. Previous work using this technique has proven its usefulness when it comes to determining atomic scale detail of the structure and hydration of small biological molecules<sup>28-35</sup>, as well as structural studies of aqueous salt solutions<sup>36-40</sup>. In this work we take a bottom-up approach to understanding the interactions of this residue by exploring the structural properties of L-aspartic acid, which we use as a model system to understand the role of aspartic acid in more complex proteins. Here L-aspartic acid has been studied in the zwitterionic form at physiological pH (henceforth referenced as ASP), in solutions of potassium chloride (KCl). The concentrations of KCl used correspond to those at which ferredoxin from the halophile, *Halobacterium Salinarium*, is native (2.5 M) and partially unfolded (0.25 M)<sup>41</sup>. Given the proposed importance of ASP in maintaining halophilic protein stability we focus in this paper on two different aspects; **(i)** the position and orientation of the water and salt ions with respect to the acidic side chain of aspartic acid. **(ii)** The interaction between water, salt and the carboxylate group of ASP.

## Method

### Neutron diffraction experiments

Neutron diffraction experiments were completed on the SANDALS diffractometer at ISIS, which probes a Q-range 0.1-50 Å<sup>-1</sup>. Neutron diffraction experiments were combined with isotopic substitution to allow labelling of individual atomic sites in a molecule and the extraction of multiple radial distribution functions ( $g(r)$ ). Protiated L-aspartic acid was purchased from Sigma Aldrich (≥ 99% purity) and a partially deuterated version from CDN isotopes (L-aspartic acid-2,3,3-d3, 98% purity), with alkyl hydrogen atoms substituted for deuterium. All solutions of aspartic acid were studied at a concentration of 0.1 M in solutions containing potassium chloride (Sigma Aldrich) at concentrations of 0.25 M and 2.5 M that are comparable with mesophilic and halophilic salt conditions. Potassium hydroxide was added set the pH at 7. The four L-aspartic acid isotopic substitution experiments completed at both high and low salt concentrations are listed in Table 1.

Upon preparation, the samples were loaded into flat-plate cans made of titanium-zirconium (TiZr) alloy, with a sample thickness of 1 mm. The collected data were normalised to a vanadium standard and corrections were made to the data for beam attenuation and multiple scattering using Gudrun<sup>42</sup>, yielding the total interference differential scattering cross section,  $F(Q)$ . The resulting  $F(Q)$  is the sum of partial structure factors  $S_{\alpha\beta}(Q)$  and can be written in terms of the atomic fraction,  $c$ , and corresponding scattering lengths,  $b$ , of atoms in the system :

$$F(Q) = \sum_{\alpha\beta} c_{\alpha} c_{\beta} b_{\alpha} b_{\beta} (S_{\alpha\beta}(Q) - 1) \quad (1)$$

where  $Q$  is the change in momentum vector by the scattered neutrons,  $Q = 4\pi \sin(\theta)/\lambda$ , and  $S_{\alpha\beta}$  represent the partial structure factor and is the Fourier-transform of the site-site radial distribution function (RDFs),  $g_{\alpha\beta}(r)$ . Integration of  $g_{\alpha\beta}(r)$  yields the coordination numbers of atom type  $\alpha$  around atoms, type  $\beta$ , at distances  $r_1$  and  $r_2$ .  $S_{\alpha\beta}(Q)$  is defined as:

$$S_{\alpha\beta}(Q) = 1 + \frac{4\pi\rho_0}{Q} \int_0^{\infty} r g_{\alpha\beta}(r) \sin(Qr) dr \quad (2)$$

where  $\rho_0$  is the atomic number density. Atomic isotopes can have different neutron scattering lengths ( $b_{\alpha}$ ), for example the neutron scattering length of hydrogen is -3.47 fm, where as that of deuterium is equal to 6.67 fm. Therefore It is possible to modify the contributions of  $S_{\alpha\beta}(Q)$  towards the measured  $F(Q)$  by modification of the

106 isotopic constituents of the scattering molecule(s). Assuming that the isotopic substitution does not alter the  
107 structure of the studied molecule, then each isotopically labelled sample yields different structural information  
108 about the solute. N isotopically different samples yields N different  $F(Q)$  data sets from which  $S_{\alpha\beta}(Q)$ 's and  
109 consequently  $g_{\alpha\beta}(r)$  can be obtained. In reality the studied system is complex and it is difficult to extract  
110 information from  $F(Q)$  alone. Therefore a computational method is required to determine all of the measured  
111 functions present in the solution.  
112

113

114

115

116 Table 1 ASP water samples for which the structure factor was measured under high and low (2.5 M and 0.25 M respectively) KCl conditions, on the SANDALS  
117 instrument.

Sample name	Contents
ASP H <sub>2</sub> O	Protiated L-aspartic acid in H <sub>2</sub> O
ASP D <sub>2</sub> O	Protiated L-aspartic acid in D <sub>2</sub> O
D-ASP H <sub>2</sub> O	Deuterated L-aspartic acid in H <sub>2</sub> O
D-ASP D <sub>2</sub> O	Deuterated L-aspartic acid in D <sub>2</sub> O

118

#### 119 **EPSR data analysis**

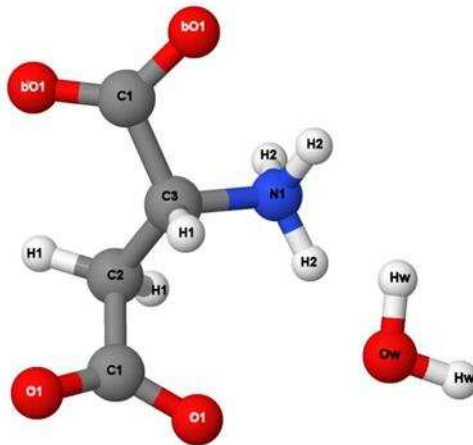
120 To extract atomic-scale information structural modelling is used with a set of constraints refined against a set of  
121 experimentally determined  $F(Q)$ , allowing the extraction of atomistic structural information about the system.  
122 Here a simulation-assisted procedure is used that has specifically been developed to convert the measured  
123 interference differential cross section to real-space, thereby yielding radial distribution functions of all atoms in  
124 the solution. This method, known as EPSR, is a variant of the reverse Monte Carlo method that attempts to  
125 produce a structural model which provides the best overall agreement with the experimentally determined  
126 diffraction data<sup>43, 44</sup>. Although EPSR does not necessarily provide the only possible interpretation it does yield a  
127 model that is consistent with the experimental data. A box of molecules was constructed at the same  
128 concentration, temperature and atomic number density as the experimentally measured samples (see SI Tables  
129 1, 2 3 and 4).

130

131

#### 132 **Naming of atoms in this paper**

133 For clarity in this paper, we refer to the different atomic components of ASP with labels, as shown in Fig. 1. We  
134 also refer to the two atomic components of water, hydrogen Hw and oxygen Ow. Furthermore potassium and  
135 chloride are labelled individually with their atomic symbol, K and Cl respectively.



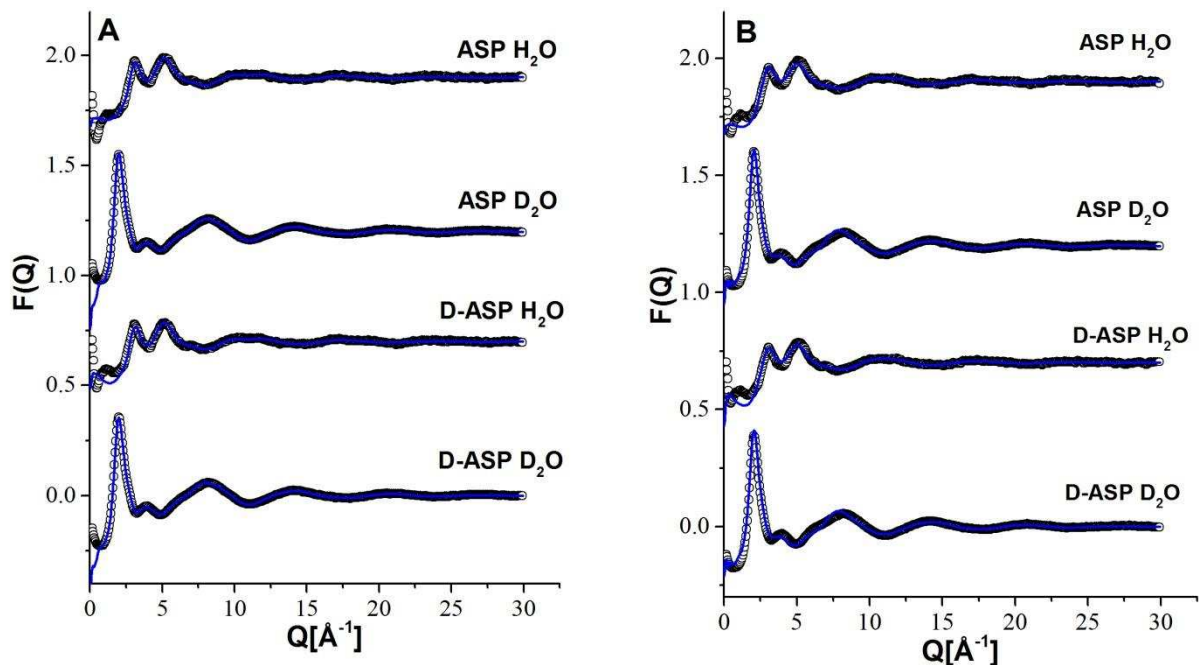
136  
137

Figure 1 Representation of the ASP and water molecules used for this study where the labels correspond to the naming throughout this study.

## 138 Results and discussion

### 139 Fits to the data

140 The measured diffraction data,  $F(Q)$ , along with the EPSR fits are shown for the solutions measured in Fig. 2,  
141 where data have been shifted along the axis vertically for clarity. The agreement between EPSR fits and the  
142 experimentally measured diffraction data is good for each sample. There is some discrepancy at low  $Q < 2 \text{ \AA}^{-1}$ . This  
143 discrepancy is due to the difficulty of removing the background and contributions from inelastic scattering in this  
144 region, caused by the presence of hydrogen in the samples. The measured  $F(Q)$  contains contributions of all  
145 partial structure factors in the solution, it is therefore not possible to observe each site-site interaction directly  
146 from the experimental data. Using the EPSR method it is possible to extract information about each individual  
147 site-site RDF from the model which is consistent with those data.



148  
149  
150  
151

Figure 2 Measured neutron  $F(Q)$ , (black circles) and fits to the data from EPSR (blue lines) of ASP acid solutions containing 2.5M KCl (left) and 0.25M KCl (right) in either  $\text{H}_2\text{O}$  or  $\text{D}_2\text{O}$  solvent. The label D-ASP indicates the use of deuterated ASP and the labels  $\text{D}_2\text{O}$  and  $\text{H}_2\text{O}$  indicate the composition of the buffer, either deuterated or protiated. The data and fits have been shifted vertically by increments of 0.5 each for improved clarity.

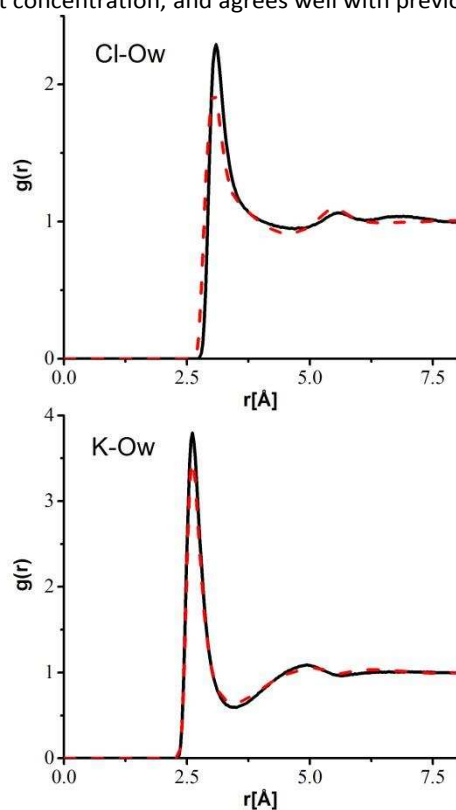
### 152 Contributions of aspartic acid to the measurement

153 Due to the low solubility of ASP, control measurements were completed on solutions containing the same ionic  
154 constituents but excluding aspartic acid. To determine how much scattering comes from ASP the  $F(Q)$  curves were

155 subtracted. The residuals for this subtraction are shown in the supporting information (SI Fig.1-3). The subtraction  
 156 indicates that, as expected, at the concentrations used in this experiments, in which ASP is soluble, the amino acid  
 157 scattering contributes only a little to the total scattering. We therefore emphasise that the results presented in  
 158 this manuscript are driven by the computer simulation, with the experimental data acting as a constraint on the  
 159 extracted structures. This is consistent with previous structural studies of biological molecules in solution in which  
 160 the solubility is limited<sup>35, 45</sup>.

161  
 162 **Ion hydration is not affected by salt concentration**

163 To investigate the hydration of the potassium and chloride ions in the solution, we present the RDFs for ion-water  
 164 interactions in Fig. 3 and S.I. Fig. 2. For each ion the water coordination numbers were calculated from the RDFs  
 165 (Table 2), according to equation 2, where  $r_2$  is the position of the first peak minimum (4.2 Å and 3.3 Å for Cl-O<sub>w</sub>  
 166 and K-O<sub>w</sub> respectively). Comparison of the RDFs for each ion at high (2.50 M) and low (0.25 M) salt concentrations  
 167 shows that both the chloride and potassium hydration shells do not change significantly with increasing ion  
 168 concentration. Correspondingly only small changes are observed in the coordination numbers (Table 2). The  
 169 insensitivity of ion hydration to salt concentration observed here is consistent with previous measurements  
 170 completed on a wide range of potassium chloride concentrations<sup>36, 37, 46</sup>. Similar to Mancinelli *et al* the position of  
 171 the RDF for Cl-O<sub>w</sub> and Cl-H<sub>w</sub> differs by 1 Å and the sharpness of the peak observed in Cl-H<sub>w</sub> corresponds to bonds  
 172 between the water oxygen and chloride ions<sup>36, 37</sup>. The Cl-H<sub>w</sub> coordination number is smaller for all solutions  
 173 compared to the Cl-O<sub>w</sub> coordination number suggesting the presence of water molecules within the hydration  
 174 shell that do not form a hydrogen bridge directly with the chloride ion. In conclusion the ion hydration remains  
 175 the same despite an increase in salt concentration, and agrees well with previous experimental results<sup>29</sup>.



176  
 177 Figure 3 Site-site RDFs of the oxygen from water (O<sub>w</sub>) around potassium (K) and chloride (Cl) ions at low (red dashed line) and high (black solid line) salt  
 178 conditions.

179 Table 2 Water-ion coordination numbers for the measured solution containing ASP, from the RDFs shown in Fig. 3.

	High KCl	Low KCl	R <sub>max</sub>	R <sub>peak</sub>
Cl-H <sub>w</sub>	4.5 ± 1.3	4.0 ± 1.2	2.8	2
Cl-O <sub>w</sub>	8.0 ± 1.2	8.3 ± 1.5	4.2	3
K-H <sub>w</sub>	16.0 ± 3.3	16.6 ± 2.8	4.1	3.3
K-O <sub>w</sub>	4.9 ± 1.4	5.0 ± 1.3	3.3	2.5

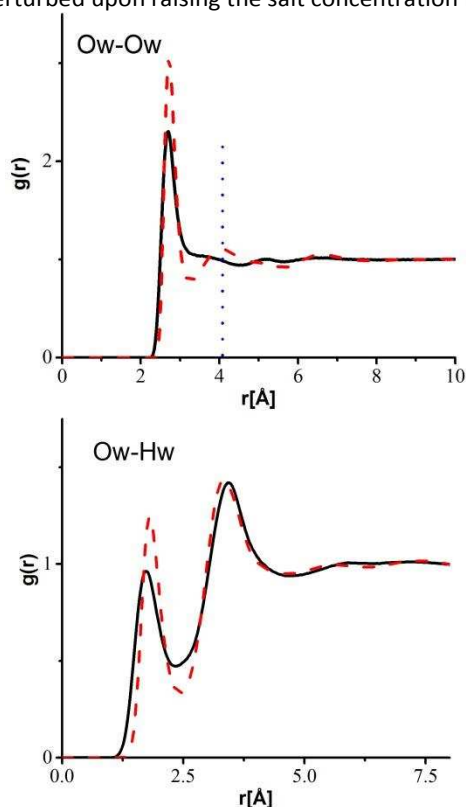
180  
 181  
 182  
 183

184

185 **Water structure is more perturbed in high KCl solution**

186 To examine the impact of KCl on water structure in the presence of ASP, RDFs for water determined by EPSR were  
 187 examined. Fig. 4, shows the RDFs for the water-water interactions ( $O_w-O_w$  and  $O_w-H_w$ ) in the ASP solutions for high  
 188 and low concentrations of KCl. The position of the peak for the  $O_w-O_w$  first coordination shell is not altered by  
 189 increasing salt concentration. The largest difference observed in the  $O_w-O_w$  RDF is the position of the second  
 190 coordination shell peak, at around 4 Å for low salt conditions, which is reduced upon increasing KCl.

191 This shift in the second coordination shell position corresponds to the disruption of the tetrahedral structure of  
 192 water and has previously been observed for high concentrations of salt including KCl as well as other solutes<sup>36, 37</sup>.  
 193 It is interesting to note that at the concentrations used here ASP does not seem to disrupt the tetrahedral  
 194 structure of water by itself. Non-disruptive behaviour of an amino acid in water has been observed in higher  
 195 concentration solutions of L-proline<sup>32</sup>. Fig. 4. also shows the  $O_w-H_w$  RDF, a slight decrease in the first  $O_w-H_w$   
 196 is observed going from 1.80 to 1.70 Å upon increasing KCl concentration. This corresponds to a strengthening of  
 197 water-water interactions upon raising the salt concentration. From these water-water RDFs it can be seen that  
 198 water is displaced by the solute molecules. The first shell coordination numbers of water were determined from  
 199 the RDFs and are listed in table 3. Regardless of peak intensity, no significant change in the water-water  
 200 coordination number of the first shell interactions are observed. In conclusion the results here suggest that the  
 201 tetrahedral structure of water is perturbed upon raising the salt concentration from 0.25M to 2.5M.



202 Figure 4 Site-site RDFs of the oxygen from water ( $O_w$ ) around the oxygen from water ( $O_w$ ) and the water hydrogen ( $H_w$ ), as determined by EPSR. Shown for  
 203 comparison for low (red dashed line) and high (black solid line) salt conditions. The blue dotted line in the  $O_w-O_w$  RDF indicates the position of the second peak  
 204 in the low salt condition.  
 205

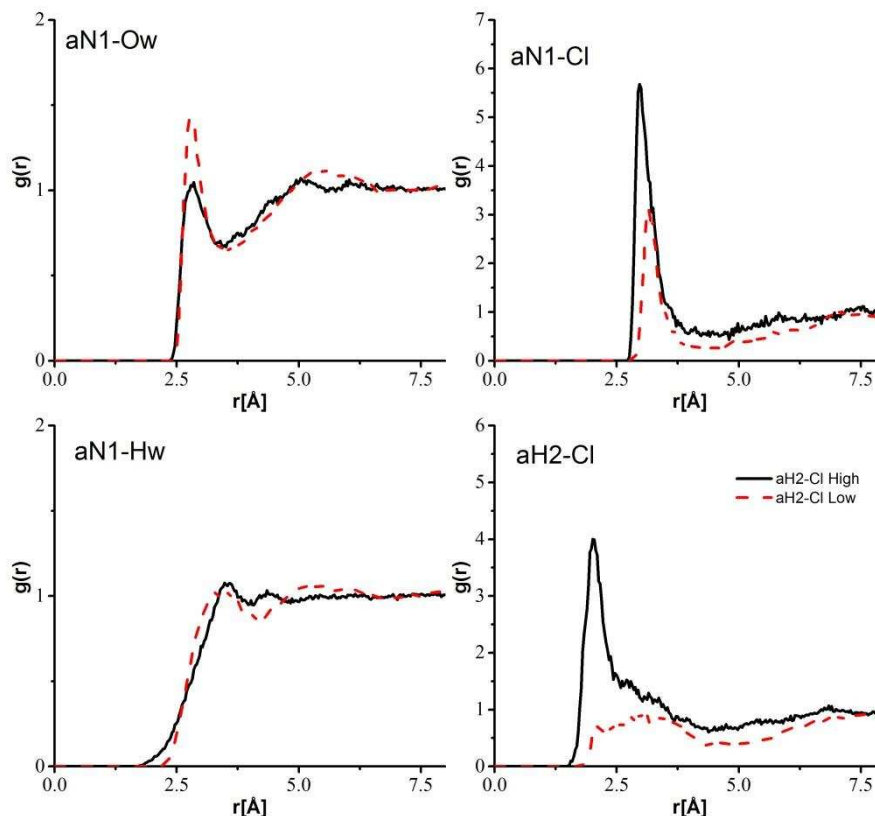
206 Table 3 Water-water coordination numbers determined from the RDFs shown in Fig. 4. For each coordination number the corresponding  
 207 maximum ( $R_{max}$ ) and the peak position ( $R_{peak}$ ) from which the coordination number was taken are shown.

	High	Low	High $R_{max}$	Low $R_{max}$	High $R_{peak}$	Low $R_{peak}$
$O_w-O_w$	$4.1 \pm 1.1$	$4.2 \pm 1$	3.2	3.2	2.5	2.5
$O_w-H_w$	$1.6 \pm 0.8$	$1.7 \pm 0.8$	2.5	2.6	1.7	1.8

208

209 **Hydration of the ASP amino group**

210 Studying a single amino acid leaves the amino group exposed to solvent water and the salt constituents. The relevant RDFs  
 211 for the amino group N1 and H2 with water are shown in Fig. 5. The first shell interactions between water and the amino  
 212 group correspond well with those previously reported (Rhys et al). Increasing salt concentration does not change the  
 213 distance of the interaction, however there is a marked decrease in the presence of water upon increasing salt.  
 214 Correspondingly an increase in the presence of chloride ions is observed (Fig. 5), indicating that the higher concentration of  
 215 ions displaces water around the amino group. This would be expected as the concentration of ions increases in the bulk  
 216 water.



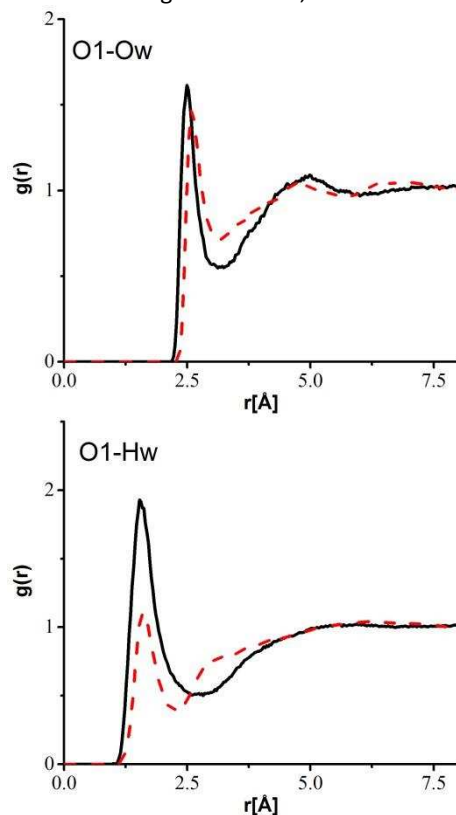
217  
 218 Figure 5 Site-site RDFs of water atoms (Ow and Hw) around the nitrogen of the ASP amino group (aN1) and chloride ions around the ASP nitrogen group  
 219 (aN1 and aH2), as determined by EPSR. Shown for low (red dashed line) and high (black solid line) salt conditions.

### 222 Hydration of the carboxylate sidechain of ASP

223 ASP is capable of forming hydrogen bonds through its charged carboxylate sidechains. In this study it was found  
 224 that the bO1 and O1 carboxyl groups have the same interactions with the solvent. *In vivo* only the O1 group is  
 225 exposed to the solvent hence we focus on the O1 carboxyl group. In order to study the effects of salt  
 226 concentration on this ability we first look at the interaction between the sidechain oxygens and the oxygen from  
 227 water (O<sub>1</sub>-O<sub>w</sub>). Fig. 6, shows the O<sub>1</sub>-O<sub>w</sub> RDF for high and low salt solutions containing ASP. The first O<sub>1</sub>-O<sub>w</sub> peak in  
 228 low salt solution is around 2.6 Å, which shifts in position to 2.5 Å upon raising the KCl concentration (see inset Fig.  
 229 5.), indicating that under higher KCl concentrations this interaction is strengthened. Investigation of the O<sub>1</sub>-H<sub>w</sub>  
 230 peak also shows a change upon increasing salt concentration, most obviously the intensity of the peak increases  
 231 with salt. Furthermore the distance of this peak is reduced from 1.6 Å to about 1.5 Å. Previously the distance  
 232 between a charged carboxylate group and the water hydrogen was determined to be around 1.68 Å for the  
 233 glutamic acid residue of glutathione<sup>33</sup>. These results suggest the presence of stronger interactions between the  
 234 water molecules and the acidic ASP. This interaction also becomes more prevalent upon increasing salt  
 235 concentration, indicated by the peak intensity observed at high KCl concentrations. The carboxylate coordination  
 236 numbers with water were determined from the areas under each peak and shown in table 4. In agreement with  
 237 the change in areas under each RDF a slight increase in the coordination of water by the carboxylate group is  
 238 observed. The hydration is decreased slightly when compared to the data previously published on the carboxylate  
 239 group of glutamine<sup>35</sup>, however, in that experiment there was no salt present which is known to affect the  
 240 hydration of amino acids. Comparison of the determined coordination numbers of the carboxylate oxygens with  
 241 those of water show that the oxygens of water are better able to coordinate other water molecules. This may be  
 242 due to a combination of geometric constraints present on the ASP carboxyl group which are not present for the



243 water oxygen and steric hindrance of water by the ASP carboxyl group. We note that for ASP the pKa ranges from  
 244 4 to 4.9 going from 0 to 5 M salt, and that this may affect the strength of the hydrogen bond between water and  
 245 ASP. In comparison for glutamic acid, the pKa ranges from 4.4 to 5.3 going from 0 to 5 M salt. Therefore under  
 246 neutral pH, ASP is the more charged acidic residue, at equivalent salt concentrations. This fact in itself may explain  
 247 the evolutionary preference for aspartic acid over glutamic acid, on the surface of halophilic proteins.



248 Figure 6 Site-site RDFs of the sidechain carboxyl oxygen from aspartic acid (O1) around the oxygen from water (O<sub>w</sub>) and the water hydrogen (H<sub>w</sub>), as  
 249 determined by EPSR. Shown for low (red dashed line) and high (black solid line) salt conditions  
 250

251 Table 4 Coordination numbers of interactions between the carboxylate group on aspartic acid and water, corresponding to the RDFs shown in figure 5. R<sub>max</sub>  
 252 and R<sub>peak</sub> are the peak position at which the coordination number was taken and the peak maxima respectively. R<sub>max</sub> high and R<sub>max</sub> low correspond to the peak  
 253 position of the high (2.5 M) and low (0.25 M) KCl containing samples.

	High	Low	R <sub>max</sub> High	R <sub>max</sub> Low	R <sub>peak</sub>
O1-O <sub>w</sub>	3.3 ± 1	2.1 ± 0.9	3.1	3.2	2.5 (low) 2.6 (high)
O1-H <sub>w</sub>	2.1 ± 1	1.1 ± 0.9	2.9	2.5	1.5

254

### 255 Interaction between the carboxylate group and potassium

256 The RDF determined for the side-chain carboxylate oxygen (O1) and potassium (K) is shown in Fig. 6. The first  
 257 coordination shell peak position remains the same for both concentrations of KCl. However upon raising the  
 258 concentration of salt the intensity decreases slightly. The corresponding coordination numbers calculated from  
 259 the RDFs shown in Fig. 6, are listed in Table 5. Contrary to the amide group, despite the 10 fold increase of KCl in  
 260 the solution there is no significant increase in the coordination of KCl around the carboxylate groups of aspartic  
 261 acid. Instead an increase in water hydration is observed around the carboxyl group (Fig. 6).

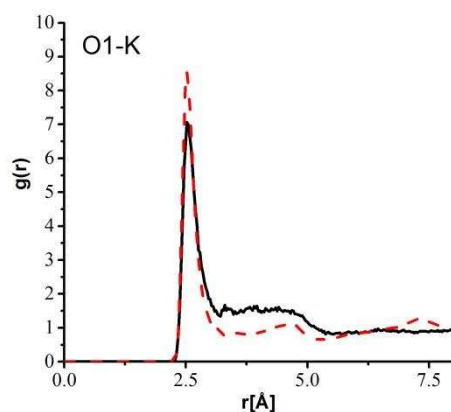


Figure 7 Site-site RDFs of potassium ions (K) around the carboxyl oxygen of aspartic acid (O1), as determined by EPSR. Shown for low (red dashed line) and high (black solid line) salt conditions.

Table 5 Coordination numbers of interactions between the oxygen on the aspartic acid carboxylate group and the potassium ion, determined from the RDFs shown in Fig. 6.

	High KCl	Low KCl	<b>Rmax</b>	<b>Rpeak</b>
<b>O1-K</b>	$0.4 \pm 0.6$	$0.3 \pm 0.5$	3.5	2.5

#### Interactions between ASP residues

At the low concentration of ASP measured here, ASP-ASP interactions are not common. This can be observed in the noise of the interactions between ASP residues as seen in the RDFs (Fig. 7). Despite this it is still possible to extract some information on the interaction between aspartic acid molecules in solution from this data. The RDFs in Fig. 7 show the interactions between the carboxylate oxygen on ASP with hydrogens H1 and H2 (see Fig. 1) on neighbouring aspartic acids. At low salt concentration, the nearest possible interaction, or  $R_{\min}$ , between two ASP residues is at a position of around 4 Å for both RDFs shown in Fig. 7. At high concentrations of KCl this value rises to just under 9 Å, suggesting a significant increase in the difference between neighbouring aspartic acid molecules. The difference in distance measured is around 5-6 Å for both RDFs in Fig. 7, which corresponds to the hydration radius of a single potassium ion. This distance would correspond to the formation of an ion bridge, preventing hydrogen bonding between neighbouring ASP residues. Therefore, the increased separation of ASP molecules at a high salt concentration may be the result of the enhanced hydration of the molecules. The hydration layer contains not only water but also ionic components, which could further inhibit the hydrogen bonding ability between two ASP residues and consequently increase the minimal distance between two ASP molecules.

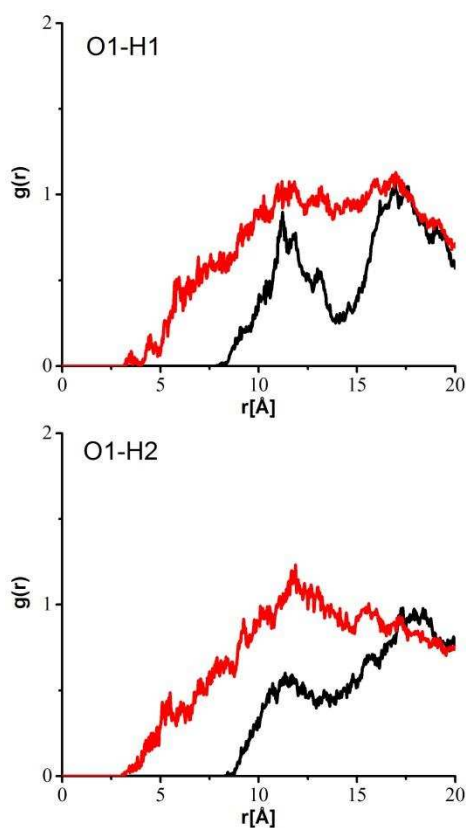


Figure 8 ASP-ASP interactions via hydrogen bonds between the carboxyl oxygen (O1) and Hydrogens on adjacent ASP residues (H1 and H2). Shown for low (red dashed line) and high (black solid line) salt conditions.

285  
286  
287

288

### 289 **Stabilisation of halophilic proteins by ASP**

290 Previously Tadeo *et al* showed that mutagenesis of only a few residues to ASP residues on the surface of a protein  
291 can lead to the formation of obligate halophiles<sup>20</sup>. More recently Ortega *et al* showed that the formation of the  
292 obligate halophile is caused by the destabilisation of the unfolded state caused by ASP and glutamic acid  
293 sidechains present in proteins isolated from halophile<sup>47</sup>. These sidechains destabilise the denatured state  
294 ensemble, mainly through cation exclusion from the protein hydration layer. The results presented here, similarly,  
295 show no increase in potassium ions around ASP upon increasing salt concentrations. Instead upon increasing KCl  
296 an increase in hydration is observed. The molecular level insight presented here is therefore in agreement with  
297 the model proposed by Ortega *et al*<sup>47</sup>, where in the unfolded state cations are excluded from the hydration shell  
298 by the action of ASP, and other, charged residues and instead are replaced by hydration water.

299

### 300 **Conclusion**

301

302 We have used a combination of neutron diffraction experiments with isotope substitution and analysis by  
303 empirical potential structure refinement to study the hydration and interactions of ASP in salt solutions. Using this  
304 approach we were able to extract atomic-scale information from the neutron diffraction data. We have found  
305 that hydration around the carboxylate group is enhanced with increasing salt concentration. We also observed a  
306 shortening of the hydrogen bond between the carboxylate oxygen and hydrogen of water upon increasing salt  
307 concentration. This tight binding of hydration water has previously been observed in crystal structures of  
308 halophilic proteins<sup>23-25</sup>. However it is not certain whether this was a true feature or an artefact of crystallisation.  
309 The solvation-stabilisation theory<sup>4</sup> states this tight binding as the possible mechanism of the stability of halophilic  
310 proteins, even under molar salt concentrations. The hydrogen bond distance between the carboxylate group and  
311 water is shorter in ASP than it is in glutamic acid<sup>33</sup>. This tighter binding of water may be due to the salt dependent  
312 pKa, under the same salt concentrations, with that of ASP being higher than that of glutamic acid. The increased  
313 affinity of water with ASP is in agreement with the theory of unfolded state destabilisation caused by the  
314 preferential exclusion of ions from the protein surface recently developed by Ortega *et al*<sup>47</sup>. Furthermore we also  
315 observed an increase in the distance between adjacent ASP residues upon increasing potassium chloride  
316 concentration. We hypothesise that this increase in distance is caused by the presence of hydrated potassium  
317 ions between different residues, indicating the presence of potassium ions in the bulk water.

318  
319  
320  
321  
322  
323  
324  
325  
326  
327  
328  
329  
330  
331  
332  
333  
334  
335  
336  
337  
338  
339  
340  
341  
342  
343  
344  
345  
346  
347  
348  
349  
350  
351  
352  
353  
354  
355  
356  
357  
358  
359  
360  
361  
362  
363  
364  
365  
366  
367  
368  
369  
370  
371  
372  
373  
374  
375  
376  
377  
378  
379

## Acknowledgements

This work was supported by the European Research Council through a grant to L.D. Experiments at the ISIS Pulsed Neutron and Muon Source were supported by a beam time allocation from the Science and Technology Facilities Council.

## References

1. G. Schäfer, *Journal of Bioenergetics and Biomembranes*, 2004, **36**, 3-4.
2. L. J. Rothschild and R. L. Mancinelli, *Nature*, 2001, **409**, 1092-1101.
3. K. M. Tych, T. Hoffmann, M. Batchelor, M. L. Hughes, K. E. Kendrick, D. L. Walsh, M. Wilson, D. J. Brockwell and L. Dougan, *Biochemical Society transactions*, 2015, **43**, 179-185.
4. D. Madern, C. Ebel and G. Zaccai, *Extremophiles : life under extreme conditions*, 2000, **4**, 91-98.
5. A. Oren, *Journal of industrial microbiology & biotechnology*, 2002, **28**, 56-63.
6. G. Schirò, Y. Fichou, F.-X. Gallat, K. Wood, F. Gabel, M. Moulin, M. Härtlein, M. Heyden, J.-P. Colletier, A. Orecchini, A. Paciaroni, J. Wuttke, D. J. Tobias and M. Weik, *Nature communications*, 2015, **6**, 6490.
7. K. Wood, M. Plazanet, F. Gabel, B. Kessler, D. Oesterhelt, D. J. Tobias, G. Zaccai and M. Weik, *P Natl Acad Sci USA*, 2007, **104**, 18049-18054.
8. G. Zaccai, *Philosophical transactions of the Royal Society of London. Series B, Biological sciences*, 2004, **359**, 1269-1275; discussion 1275, 1323-1268.
9. P. Ball, *Chemical reviews*, 2008, **108**, 74-108.
10. A. Oren, *Saline systems*, 2008, **4**, 2.
11. H. Larsen, *Advances in Microbial Physiology*, 1967, **1**, 97-132.
12. W. Stoeckenius, R. H. Lozier and R. A. Bogomolni, *Biochimica et Biophysica Acta (BBA) - Reviews on Bioenergetics*, 1979, **505**, 215-278.
13. D. Oesterhelt and J. Tittor, *Trends in Biochemical Sciences*, 1989, **14**, 57-61.
14. M. Mevarech, F. Frolow and L. M. Gloss, *Biophysical Chemistry*, 2000, **86**, 155-164.
15. G. Graziano and A. Merlino, *Biochimica et biophysica acta*, 2014, **1844**, 850-858.
16. J. A. Winter, P. Christofi, S. Morroll and K. A. Bunting, *BMC structural biology*, 2009, **9**, 55.
17. R. Deole, J. Challacombe, D. W. Raiford and W. D. Hoff, *The Journal of biological chemistry*, 2013, **288**, 581-588.
18. K. L. Britton, P. J. Baker, M. Fisher, S. Ruzheinikov, D. J. Gilmour, M.-J. Bonete, J. Ferrer, C. Pire, J. Esclapez and D. W. Rice, *P Natl Acad Sci USA*, 2006, **103**, 4846-4851.
19. D. Madern, C. Pfister and G. Zaccai, *European Journal of Biochemistry*, 2008, **230**, 1088-1095.
20. X. Tadeo, B. López-Méndez, T. Trigueros, A. Laín, D. Castaño and O. Millet, *PLoS biology*, 2009, **7**, e1000257.
21. A. Razvi and J. M. Scholtz, *Biochemistry*, 2006, **45**, 4084-4092.
22. G. Zaccai, *Biopolymers*, 2013, **99**, 233-238.
23. S. Arai, Y. Yonezawa, N. Okazaki, F. Matsumoto, C. Shibazaki, R. Shimizu, M. Yamada, M. Adachi, T. Tamada, M. Kawamoto, H. Tokunaga, M. Ishibashi, M. Blaber, M. Tokunaga and R. Kuroki, *Acta crystallographica. Section D, Biological crystallography*, 2015, **71**, 541-554.
24. R. Talon, N. Coquelle, D. Madern and E. Girard, *Frontiers in microbiology*, 2014, **5**, 66.
25. F. Frolow, M. Harel, J. L. Sussman, M. Mevarech and M. Shoham, *Nature structural biology*, 1996, **3**, 452-458.
26. O. Carugo and K. Djinović-Carugo, *Journal of Applied Crystallography*, 2013, **47**, 458-461.
27. D. Fusco, J. J. Headd, A. De Simone, J. Wang and P. Charbonneau, *Soft matter*, 2014, **10**, 290-302.
28. S. K. Callear, A. Johnston, S. E. McLain and S. Imberti, *The Journal of chemical physics*, 2015, **142**, 014502.
29. S. Busch, L. C. Pardo, W. B. O'Dell, C. D. Bruce, C. D. Lorenz and S. E. McLain, *Physical chemistry chemical physics : PCCP*, 2013, **15**, 21023-21033.
30. S. Busch, C. D. Bruce, C. Redfield, C. D. Lorenz and S. E. McLain, *Angewandte Chemie*, 2013, **52**, 13091-13095.
31. S. E. McLain, A. K. Soper and A. Watts, *European biophysics journal : EBJ*, 2008, **37**, 647-655.
32. S. E. McLain, A. K. Soper, A. E. Terry and A. Watts, *The journal of physical chemistry. B*, 2007, **111**, 4568-4580.
33. E. Scoppola, A. Sodo, S. E. McLain, M. A. Ricci and F. Bruni, *Biophysical journal*, 2014, **106**, 1701-1709.
34. A. J. Johnston, Y. R. Zhang, S. Busch, L. C. Pardo, S. Imberti and S. E. McLain, *The journal of physical chemistry. B*, 2015, **119**, 5979-5987.
35. N. H. Rhys, A. K. Soper and L. Dougan, *The journal of physical chemistry. B*, 2012, **116**, 13308-13319.
36. R. Mancinelli, A. Botti, F. Bruni, M. A. Ricci and A. K. Soper, *The journal of physical chemistry. B*, 2007, **111**, 13570-13577.

- 380 37. R. Mancinelli, A. Botti, F. Bruni, M. A. Ricci and A. K. Soper, *Physical chemistry chemical physics : PCCP*,  
381 2007, **9**, 2959-2967.
- 382 38. T. G. A. Youngs, J. D. Holbrey, C. L. Mullan, S. E. Norman, M. C. Lagunas, C. D'Agostino, M. D. Mantle, L. F.  
383 Gladden, D. T. Bowron and C. Hardacre, *Chem Sci*, 2011, **2**, 1594-1605.
- 384 39. A. J. Johnston, Y. P. Zhang, S. Busch, L. C. Pardo, S. Imberti and S. E. McLain, *Journal of Physical Chemistry*  
385 *B*, 2015, **119**, 5979-5987.
- 386 40. T. Murphy, R. Hayes, S. Imberti, G. G. Warr and R. Atkin, *Physical Chemistry Chemical Physics*, 2014, **16**,  
387 13182-13190.
- 388 41. A. K. Bandyopadhyay and H. M. Sonawat, *Biophysical journal*, 2000, **79**, 501-510.
- 389 42. A. K. Soper, *Mol Phys*, 2009, **107**, 1667-1684.
- 390 43. A. K. Soper, *Chem Phys*, 1996, **202**, 295-306.
- 391 44. A. K. Soper, *J Mol Liq*, 1998, **78**, 179-200.
- 392 45. N. H. Rhys, A. K. Soper and L. Dougan, *The journal of physical chemistry. B*, 2015, **119**, 15644-15651.
- 393 46. P. Gallo, D. Corradini and M. Rovere, *J Mol Liq*, 2014, **189**, 52-56.
- 394 47. G. Ortega, T. Diercks and O. Millet, *Chemistry & biology*, 2015, **22**, 1597-1607.

395